Supporting information

One-step formation of composite inorganic interphases for stable zinc metal anodes

Xinchun Song[a], Jingliang Jiang[b], Yifang Zhang[b], Gan Li[a], Zhengquan Xiao[a], En Gao[a], Yongtao Li[a,c*] and Zhipeng Jiang[a,c*]

[a] School of Materials Science and Engineering, Anhui University of Technology, Maanshan 243002, China.

[b] Chengdu Aircraft industrial (Group) Co.LTD, Chengdu 610091, China.

[c] Key Laboratory of Efficient Conversion and Solid-state Storage of Hydrogen & Electricity of Anhui Province, Maanshan 243002, China.

[*] Corresponding author.

E-mail: liyongtao@ahut.edu.cn; jzp1994@ahut.edu.cn.

1. Experimental section

Electrolyte preparation

A 1 M $ZnSO_4$ aqueous electrolyte was prepared by dissolving $ZnSO_4$ (Aladdin, >99%) in deionized water under magnetic stirring until a homogeneous solution was obtained.

Preparation of treated Zn anode

Zn foils with a diameter of 14 mm were immersed in an aqueous 1 M $LiPF_6$ solution and subsequently transferred to a sealed reactor for hydrothermal treatment at 60 °C for 1 h. After the reaction, the samples were collected and thoroughly rinsed with deionized water and ethanol several times to remove residual species, followed by drying before further use.

Synthesis of $NH_4V_4O_{10}$ cathode material

$NH_4V_4O_{10}$ was synthesized through a hydrothermal method. Briefly, NH_4VO_3 (584.95 mg) and sodium dodecylbenzenesulfonate (SDBS, 0.2 g) were dissolved in 60 mL of deionized water and stirred for 30 min to obtain a uniform solution. Subsequently, 2.5 mL of diluted sulfuric acid was slowly introduced under continuous stirring, and the mixture was further stirred for 30 min until a transparent orange-yellow solution formed. The precursor solution was then transferred to a Teflon-lined autoclave and heated at 200 °C for 24 h. After cooling to room temperature, the obtained green precipitate was collected by centrifugation, washed repeatedly with deionized water and ethanol, and finally dried at 80 °C for subsequent use.

Electrochemical measurements

The cathode slurry was prepared by mixing $NH_4V_4O_{10}$, Super P (DoDoChem), and polyvinylidene fluoride (PVDF, DoDoChem) in a mass ratio of 7:2:1. The mixture was dispersed in 1-methyl-2-pyrrolidone (NMP, Innochem, 99.9%) and ground until a homogeneous slurry was obtained. The slurry was uniformly coated onto titanium foil (20 μm thick) and dried at 80 °C. The electrode was then punched into circular disks with a diameter of 8 mm, giving an active material loading of approximately 1.2 mg cm^{-2}. For high–mass loading electrodes, $NH_4V_4O_{10}$, Super P, and polytetrafluoroethylene (PTFE, Guangdong Canrd New Energy Technology Co., Ltd.) were blended at a weight ratio of 7:2:1. The resulting slurry was coated onto stainless steel mesh current collectors (1.2 cm^2) and dried at 80 °C, resulting in an areal active material loading of about 3.3 mg cm^{-2}. Zn–$NH_4V_4O_{10}$ full cells were assembled using $NH_4V_4O_{10}$ as the cathode, Zn foil (99.99%, 14 mm diameter, 100 μm thickness) as the anode, and a Whatman GF/D glass fiber separator (19 mm diameter). For high-loading cathode tests, Zn foil with a thickness of 10 μm was used as the anode. Galvanostatic charge–discharge measurements were conducted within a voltage window of 0.2–1.8 V. Zn–Cu half cells were assembled using Cu foil (16 mm diameter, 12 μm thickness) as the working electrode. Additionally, Zn–Zn symmetric cells, Zn–Cu half cells, and Zn–$NH_4V_4O_{10}$ full cells were assembled for electrochemical evaluation. All CR2032 coin cells were tested at 25 °C using a Neware battery testing system (Shenzhen Neware Technology Co., Ltd.).

Characterizations

The surface morphology of the treated Zn and the cycled Zn electrodes was examined using scanning electron microscopy (SEM, Zeiss Sigma 300). Using Bruker Dimension Icon Atomic Force Microscope (AFM) to test the surface morphology and Young's modulus of Zn foil. The chemical composition and surface states were analyzed by X-ray photoelectron spectroscopy (XPS, Thermo Scientific K-Alpha). Time-of-flight secondary ion mass spectrometry (TOF-SIMS, ION-TOF GmbH TOF-SIMS IV) was employed to investigate the surface chemical distribution

of the treated Zn electrode, with a sputtering duration of 800 s. X-ray diffraction (XRD) analysis of the soaked Zn anodes was conducted using a MiniFlex600 diffractometer to identify crystalline phases. Use the HE-CA200 water drop contact angle measuring instrument to test the contact angle between Zn foil and the electrolyte.

Electrochemical measurements

Electrochemical tests were performed on a CHI660E electrochemical workstation. Linear sweep voltammetry (LSV) measurements were conducted in Zn–Cu half-cells at a scan rate of 1 mV s^{-1}. The Zn^{2+} transference number was determined at 25 °C using Zn–Zn symmetric cells based on the Bruce–Vincent method.[1] The equation used is:

$$t_+ = \frac{I_{ss}(\Delta V - R_0 I_0)}{I_0(\Delta V - R_{ss} I_{ss})}$$

Chronoamperometry (CA) measurements were carried out using Zn–Zn symmetric cells under a constant overpotential of −150 mV for 300 s. Electrochemical impedance spectroscopy (EIS) tests were performed on Zn–$NH_4V_4O_{10}$ cells. To evaluate the temperature dependence of interfacial kinetics, Zn–Zn symmetric cells were tested over a temperature range from 10 to 50 °C. The SEI resistance values were extracted from fitted EIS spectra and further analyzed using the Arrhenius equation[2]:

$$K = Aexp(-E_a/RT)$$

Theoretical Calculations

Density functional theory (DFT) calculations were performed using the Vienna Ab initio Simulation Package (VASP)[3,4], leveraging the Perdew-Burke-Ernzerhof (PBE)[5] exchange-correlation functional within the generalized gradient approximation (GGA)[6] framework. To eliminate interactions between periodically repeated layers, a vacuum space of 15 Å was introduced. The DFT-D3[7] method with Becke-Johnson damping was employed to account for van der Waals interactions. The projected augmented wave (PAW)[8] method was adopted alongside a plane-wave basis set with a cutoff energy of 500 eV. Simulations were performed using a 2*2*1 k-point grid for sampling the Brillouin zone. The Zn, ZnF_2, ZnO, and (002) surface were specifically constructed to investigate the adsorption behavior of Zn^{2+}, H_2O, and TFEA. The adsorption energy (E_{ads}) was calculated using the following formula:

$$E_{ads} = E_{total(Molecule+Surface)} - E_{Surface} - E_{Molecule}$$

where $E_{total(Molecule+Surface)}$, $E_{Surface}$, and $E_{Molecule}$ are the total energies of the adsorption system, the clean surface, and the isolated molecule, respectively.

2. Supporting Figures

1. $LiPF_6+H_2O \rightarrow LiF+POF_3+2HF$
2. $POF_3+3H_2O \rightarrow H_3PO_4+3HF$
3. $Zn+H_2O \rightarrow ZnO+H_2\uparrow$
4. $Zn+2HF \rightarrow ZnF_2+H_2\uparrow$
5. $3Zn+2H_3PO_4 \rightarrow Zn_3(PO_4)_2+3H_2\uparrow$

Fig. S1 Chemical reactions occurring on the Zn foil during hydrothermal treatment with $LiPF_6$.

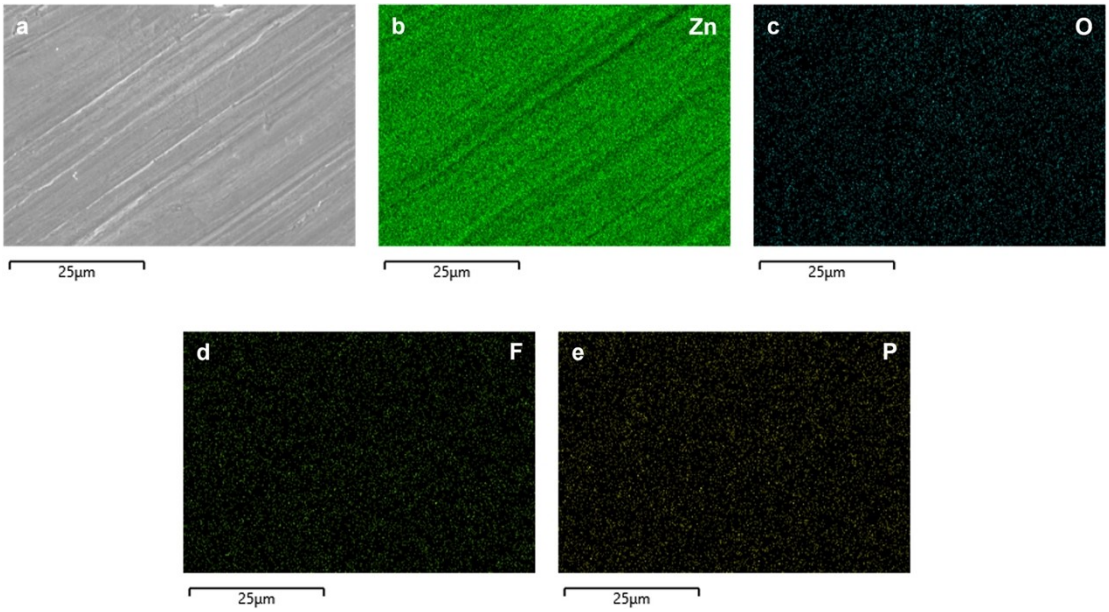

Fig. S2 (a) SEM front-view image of the treated Zn surface, accompanied by EDX elemental distribution maps for (b) Zn, (c) O, (d) F, and (e) P.

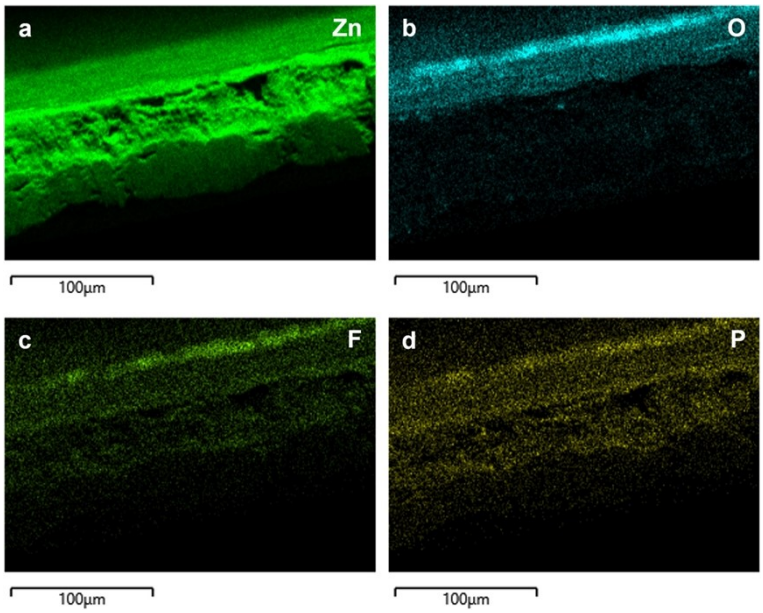

Fig. S3 SEM cross-sectional EDX elemental distribution maps of treated Zn: (a) Zn, (b) O, (c) F, and (d) P.

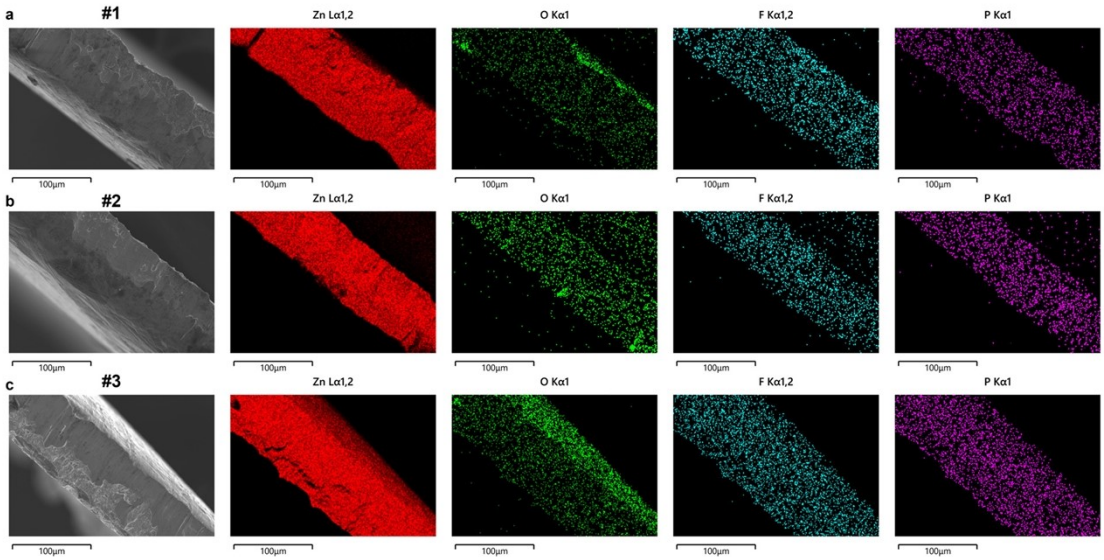

Fig. S4 SEM cross-sectional images of treated Zn and corresponding EDX elemental distribution maps for different batches: (a) Batch #1, (b) Batch #2, and (c) Batch #3.

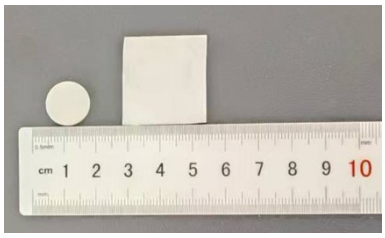

Fig. S5 Photographs of Zn foil and large-area electrodes following hydrothermal treatment.

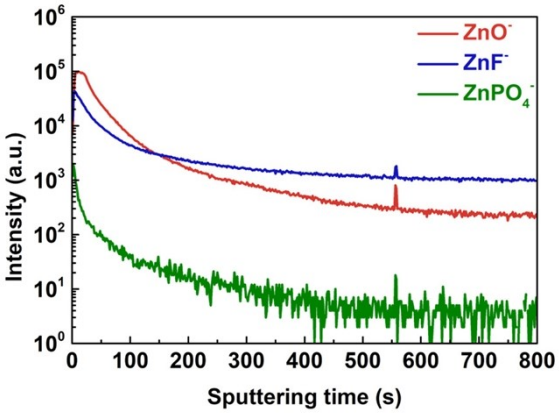

Fig. S6 Normalized TOF-SIMS depth profiles of treated Zn.

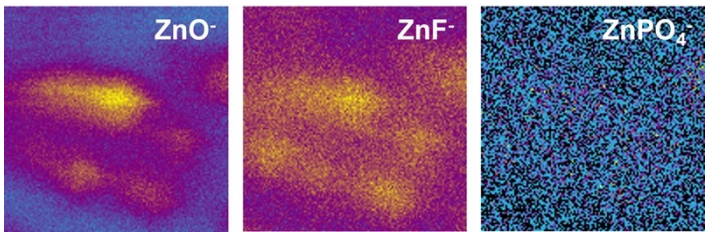

Fig. S7 Cross-profile images of TOF-SIMS depth sputtering of treated Zn.

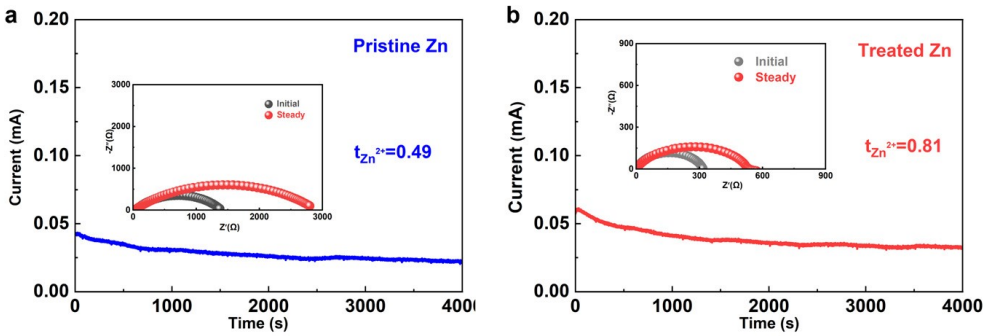

Fig. S8 Zn^{2+} transference numbers of Zn-Zn symmetric cells assembled with different Zn foils: (a) pristine Zn; (b) treated Zn.

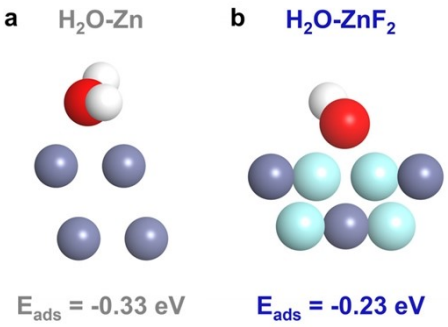

Fig. S9 Comparison of adsorption energies for (a) H_2O–Zn and (b) H_2O–ZnF_2.

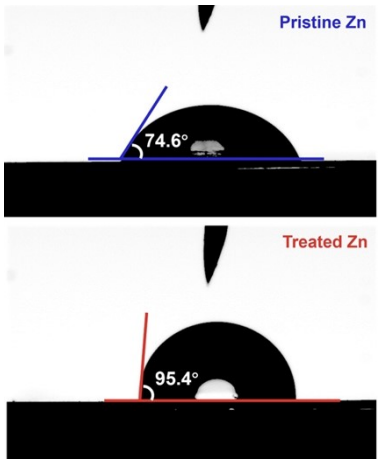

Fig. S10 Contact angles of the electrolyte on different Zn foils: (a) pristine Zn; (b) treated Zn.

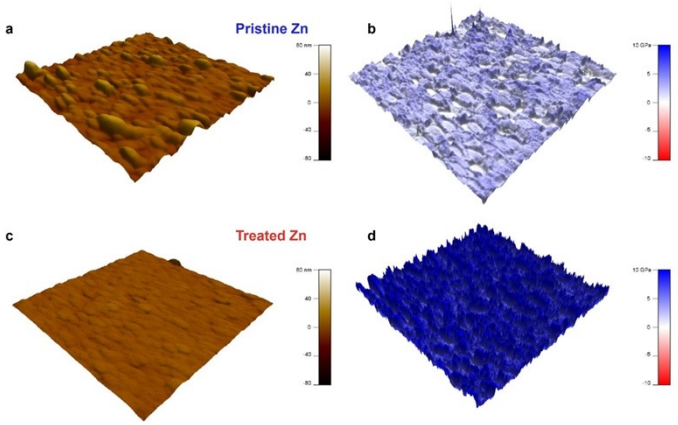

Fig. S11 AFM characterization of Zn foils. Topography images (a, c) and corresponding surface Young's modulus maps (b, d) of (a, b) pristine Zn and (c, d) treated Zn.

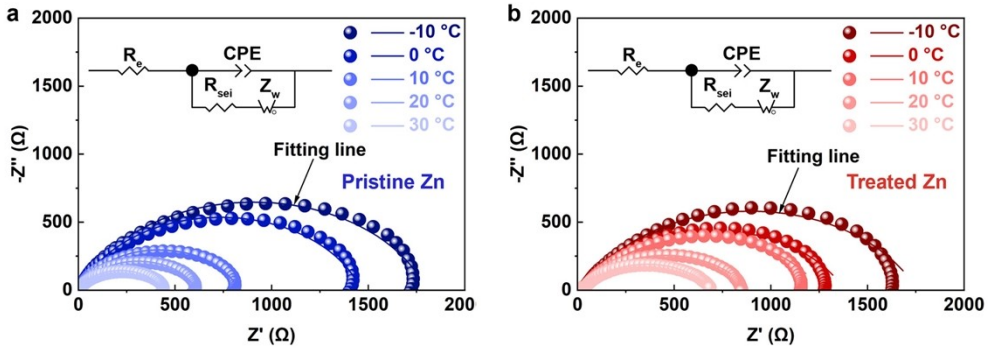

Fig. S12 EIS plots of Zn–Zn symmetric cells with (a) pristine Zn and (b) treated Zn at different temperatures.

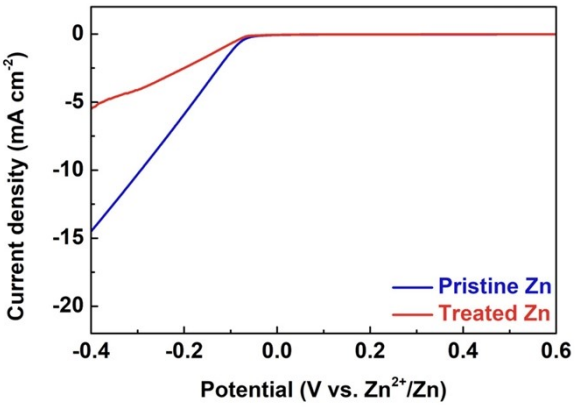

Fig. S13 LSV curves of different Zn anodes.

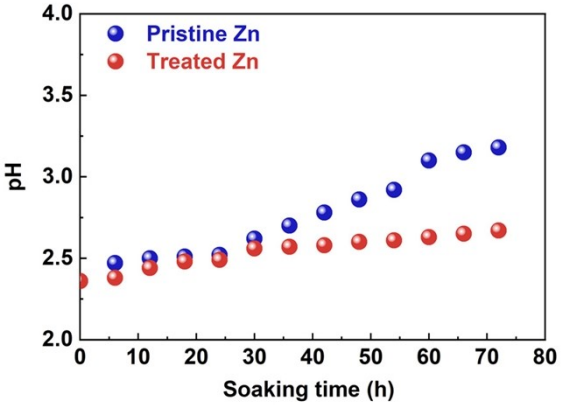

Fig. S14 Temporal evolution of electrolyte pH values measured after different soaking durations.

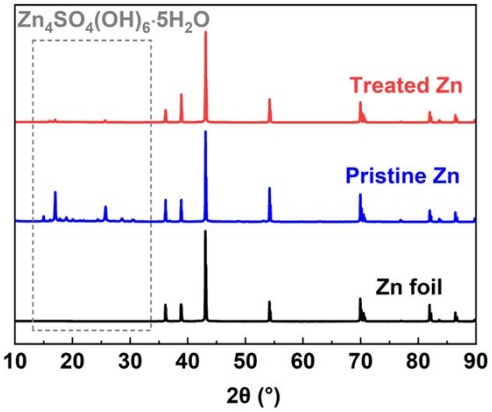

Fig. S15 X-ray diffraction patterns of various Zn anodes after immersion in the electrolyte for 3 days.

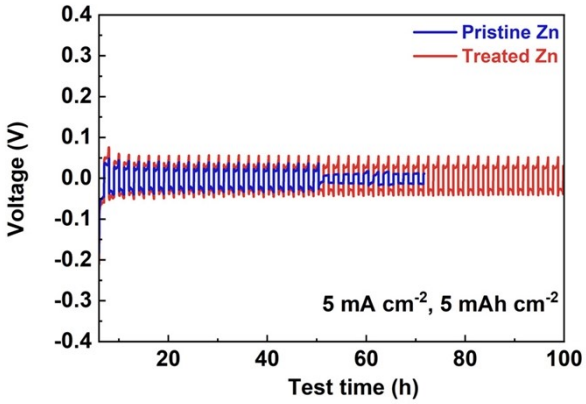

Fig. S16 Cycling performance comparison of Zn-Zn symmetric cells using different Zn anodes (5 mA cm^{-2}, 5 mAh cm^{-2}).

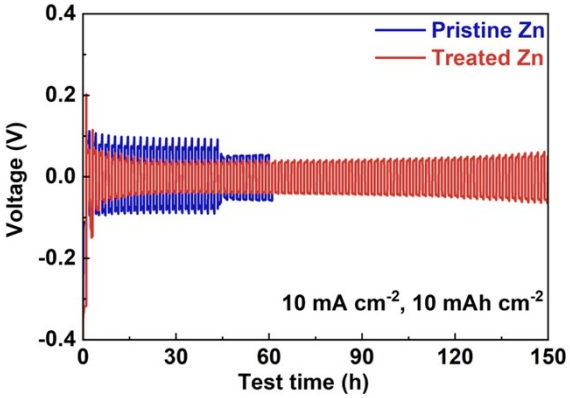

Fig. S17 Cycling performance comparison of Zn-Zn symmetric cells using different Zn anodes (10 mA cm^{-2}, 10 mAh cm^{-2}).

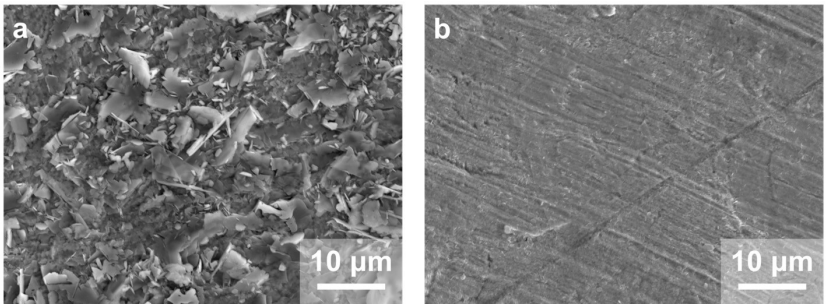

Fig. S18 SEM images of cycled Zn anodes: (a) pristine Zn and (b) treated Zn. (Cycle conditions: 1 mA cm^{-2}, 1 mAh cm^{-2}, 50 h)

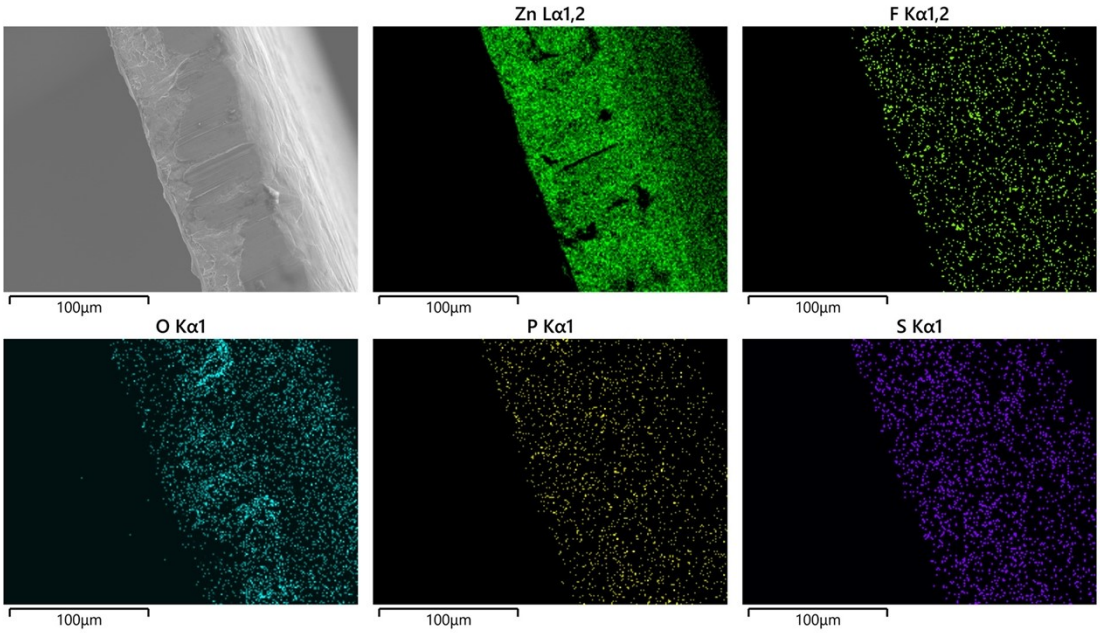

Fig. S19 SEM cross-sectional images of cycled Zn and corresponding EDX elemental distribution maps. (Cycle conditions: 5 mA cm^{-2}, 0.5 mAh cm^{-2}, 500 cycles)

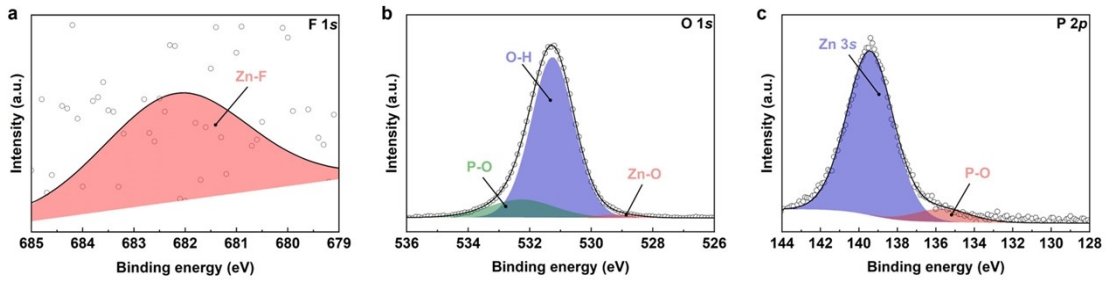

Fig. S20 XPS spectra of cycled Zn showing (a) F 1*s*, (b) O 1*s* and (d) P 2*p*. (Cycle conditions: 5 mA cm^{-2}, 0.5 mAh cm^{-2}, 500 cycles)

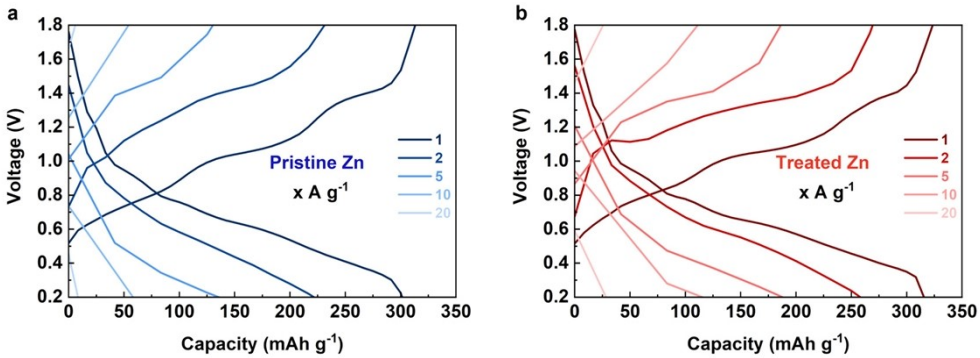

Fig. S21 Voltage profiles of Zn–$NH_4V_4O_{10}$ cells during rate testing using (a) pristine Zn and (b) treated Zn.

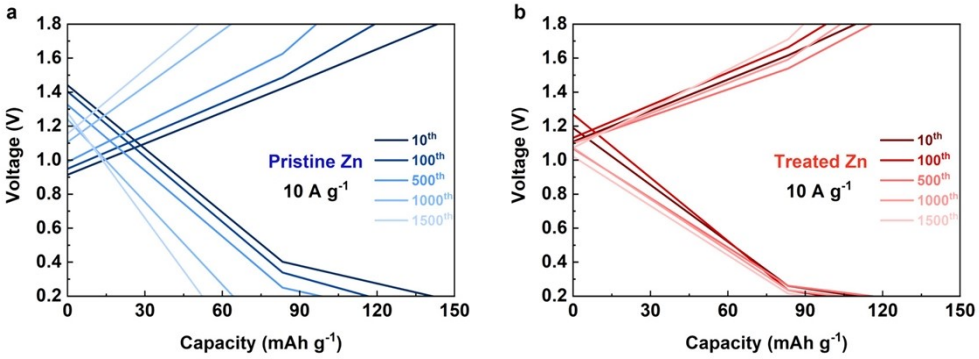

Fig. S22 Voltage profiles of Zn–$NH_4V_4O_{10}$ cells during cycling testing using (a) pristine Zn and (b) treated Zn.

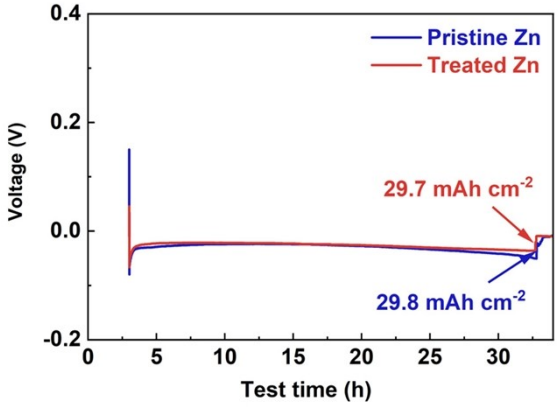

Fig. S23 Areal capacity comparison of Zn–Cu half-cells prepared using various Zn foils during continuous discharge testing. The measurements were conducted at a current density of 1 mA cm^{-2}.

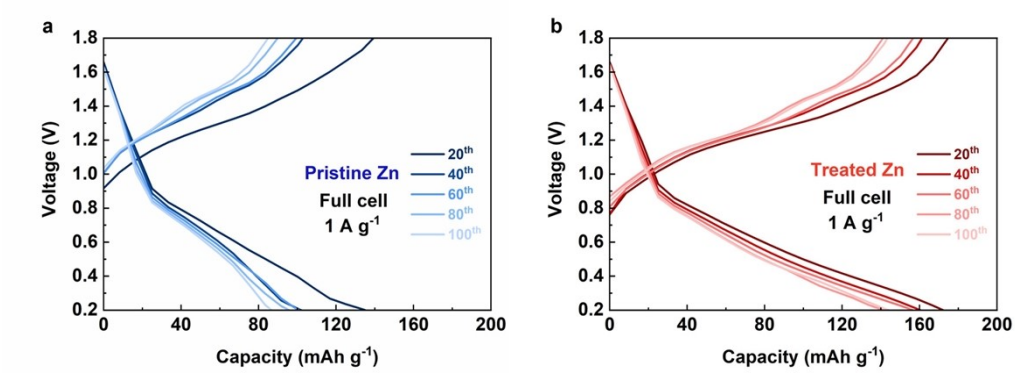

Fig. S24 Voltage profiles of Zn–$NH_4V_4O_{10}$ full cells during cycling testing using (a) pristine Zn and (b) treated Zn.

Table S1. Comparison of the performance of Zn-Zn symmetric cells assembled with different coated Zn.

Coated Zn	Test condition	Cycling time	Reference
α-B@Zn	0.5 mA cm^{-2}, 0.25 mAh cm^{-2}	2200 h	*Adv. Funct. Mater.* **2025**, *35*, e2507725
Py@Zn	1 mA cm^{-2}, 1 mAh cm^{-2}	2850 h	*Adv. Energy Mater.* **2025**, *15*, e03193
ASCZ-Zn	0.5 mA cm^{-2}, 0.5 mAh cm^{-2}	3500 h	*J. Energy Chem.* **2026**, *117*, 635
PRGA@Zn	1 mA cm^{-2}, 1 mAh cm^{-2}	2000 h	*Chem. Commun.* **2026**, *62*, 5956
Zn@CHP	5 mA cm^{-2}, 1 mAh cm^{-2}	1200 h	*Green Chem.* **2026**, *28*, 4972
ATP-Zn	0.25 mA cm^{-2}, 0.05 mAh cm^{-2}	1300 h	*J. Mater. Chem. A* **2026**, 10.1039/D5TA08687F
PAD-NAF@Zn	1 mA cm^{-2}, 1 mAh cm^{-2}	1000 h	*Small*, **2026**, *22*, e13131
SPEEK-BN@Zn	1 mA cm^{-2}, 1 mAh cm^{-2}	1800 h	*Small*, **2026**, *22*, e00003
Treated Zn	**5 mA cm^{-2}, 1 mAh cm^{-2}**	**>1600 h**	**Our work**

Reference

[1] G. Qu，H. Wei, S. Zhao, *Adv. Mater.*, 2024, **36**, 2400370

[2] F. Cheng, Angew, Chem, *Angew. Chem. Int. Ed*., 2025, **64**, e202415853.

[3] G. Kresse, J. Furthmüller, *Phys. Rev. B,* 1996, **54**, 11169–11186.

[4] G. Kresse, J. Furthmüller, *Comput. Mater. Sci.,* 1996, **6**, 15–50.

[5] P. Kraus, *J. Chem. Theory Comput.,* 2021, **17**, 5651–5660.

[6] S. Grimme, *J. Comput. Chem.,* 2006, **27**, 1787–1799.

[7] S. Grimme, J. Antony, S. Ehrlich, H. Krieg, *J. Chem. Phy.,* 2010, **132**, 154104.

[8] E. Torres, T. P. aloni, *Comput. Mater. Sci.,* 2020, **171**, 109237.